Quaternary Geochronology 79 (2024) 101473

Contents lists available at ScienceDirect

Quaternary Geochronology

journal homepage: www.elsevier.com/locate/quageo

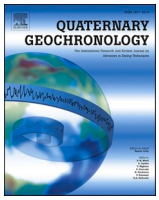

Investigating the potential of African land snail shells (Gastropoda: Achatininae) for amino acid geochronology☆

Chloë Baldreki [a,*], Andrew Burnham [a], Martina Conti [a], Lucy Wheeler [a], Michael J. Simms [b], Lawrence Barham [c], Tom S. White [d], Kirsty Penkman [a]

[a] Department of Chemistry, University of York, UK
[b] Senior Curator of Geology, National Museums Northern Ireland
[c] Department of Archaeology, Classics and Egyptology, University of Liverpool, UK
[d] Principal Curator, non-Insect Invertebrates, Natural History Museum, London, UK

ARTICLE INFO

Keywords:
AAR
Racemisation
Quaternary
Dating
Gastropod shell
Africa

ABSTRACT

Aragonitic calcium carbonate ($CaCO_3$) terrestrial mollusc shells with complex shell microstructures, such as those in the African subfamily Achatininae, have the potential to be used to build amino acid geochronologies across the African continent. However, as different microstructural shell layers are likely to have different protein compositions, sampling strategies need to be developed to identify the most appropriate shell portion to target. To test possible variability in protein degradation rates between microstructural layers, sampling of a single microstructural shell layer (the 'nacreous' layer) was compared to sampling all three aragonitic layers ('3AL') in modern and fossil shells. Reliable isolation of the nacreous layer in all samples proved impractical, and additional complications arose due to mineral diagenesis induced by sampling with a drill. Pleistocene fossils of *Lissachatina* sp. and modern specimens of *Achatina tavaresiana* Morelet, 1866 were shown to have an intra-crystalline protein fraction. The 3AL shell portion adhered more closely to closed-system behaviour in heated modern, and fossil, samples. The intra-crystalline protein degradation (IcPD) patterns of Achatininae fossil samples were not consistent with IcPD under forced degradation experiments at high temperatures in the laboratory. However, reliable degradation trends were observed in the 3AL shell portion, demonstrating the potential of fossil achatinids for building relative amino acid geochronologies across Africa.

1. Introduction

The shells of non-marine molluscs have potential to be used for amino acid geochronologies (AAG), a dating technique which exploits the time-dependent diagenesis of proteins (e.g., racemisation, hydrolysis and degradation of amino acids) contained within biominerals (Abelson, 1955; Hare and Mitterer, 1967; Penkman et al., 2008; Hearty and Kaufman, 2009). AAG studies within the African continent to date have primarily focussed on ostrich eggshell (e.g., Brooks et al., 1990; Miller et al., 1992; Murray-Wallace et al., 2015), with a paucity of studies based on other biominerals. Globally, the shells of terrestrial gastropod molluscs have been used for AAG in various locations (e.g. *Actinella nitidiuscula* in Madeira (New et al., 2019); *Trochoidea seetzeni* in Israel (Goodfriend, 1991); *Cerion* sp. in the Bahamas (Hearty and Kaufman, 2009); *Poecilozonites* in Bermuda (Hearty and Olson, 2010); *Rabdotus mooreanus* in the USA (Ellis et al., 1996) and a variety of taxa in Europe e.g. *Theba* sp. in the Canary Islands (Ortiz et al., 2006) and *Trichia* sp. and *Cepaea* sp. in the UK (Bowen et al., 1989)), but in Africa very few studies based on terrestrial gastropod molluscs have been published (e.g. *Trophidophora* sp. land snails in South Africa (Roberts et al., 2008). There is therefore scope for developing amino acid geochronologies using understudied biominerals, such as the shells of common land snail species in the subfamily Achatininae, which occur across Africa (Fontanilla, 2010) and include regions where ostrich eggshell is not present.

Achatininae is a subfamily of medium-large land snails native to the African continent. The sizable shells (up to 20 cm in some species) of achatinids have an extensive fossil record (Solem, 1979) that extends back at least as far as the Miocene (Pickford, 1995, 2008), with some

☆ "For the purpose of open access, the author has applied a Creative Commons Attribution (CC BY) licence to any Author Accepted Manuscript version arising from this submission."

* Corresponding author.
E-mail address: chloe.baldreki@york.ac.uk (C. Baldreki).

https://doi.org/10.1016/j.quageo.2023.101473
Received 20 May 2023; Received in revised form 21 September 2023; Accepted 25 September 2023
Available online 29 September 2023

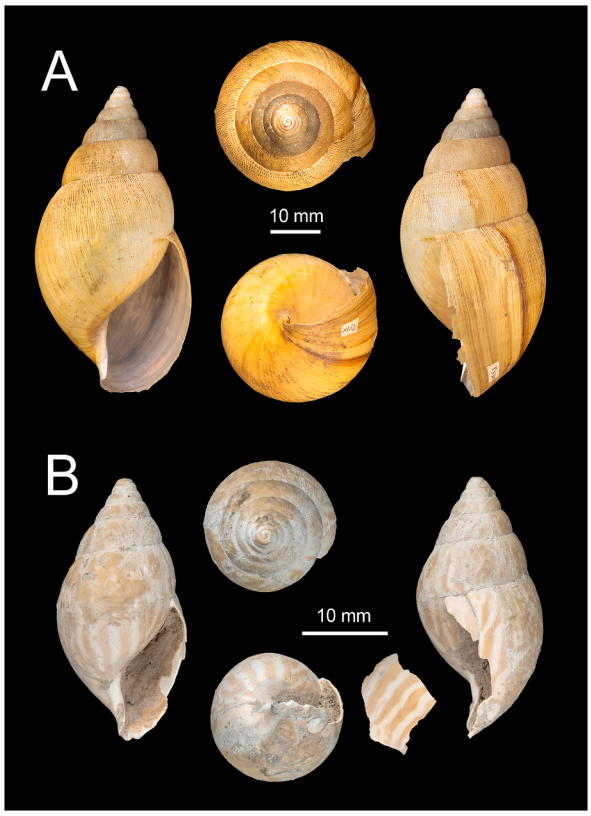

Fig. 1. A - *Achatina tavaresiana* Morelet, 1866 (syntype, NHMUK, 1893.2.4.151). B - *Lissachatina* sp. (fossil specimen PK.S19.4, from Palaeolake Kafue (Site 19) near Twin Rivers kopje).

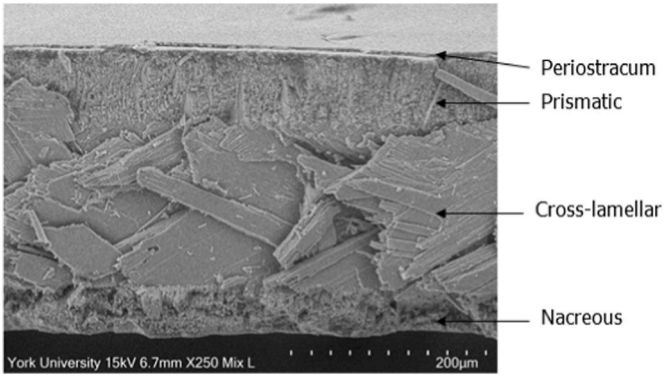

Fig. 2. SEM image (×250) of a modern *Achatina tavaresiana* shell, showing four microstructural layers: the periostracum, prismatic, cross-lamellar and nacreous.

probable but contested records from the Eocene (Neubert and van Damme, 2012; Pickford et al., 2014; Hammouda et al., 2017). Achatinid fossils have the potential to provide both palaeoecological and palaeoclimatic data (White et al., 2017; Taylor et al., 2011), as well as age estimation, for example via radiocarbon dating (e.g., Wojcieszak et al., 2023 and references therein) and AAG. Species of the genus *Achatina* (Fig. 1A) have a current distribution across sub-Saharan West Africa (Fontanilla, 2010; *contra* older works such as Hodasi, 1984; Raut and Barker, 2002), while those of the genus *Lissachatina* (Fig. 1B) occur in central-eastern Africa (Fontanilla, 2010). Achatinids occupy a wide range of habitats, from equatorial rainforest to open savannah and the semi-desert environments of south and southwest Africa. Some, most notably *Lissachatina fulica* Bowdich, 1882, have become invasive crop-pests where introduced in many other parts of the world (Vijayan et al., 2022), leading to the suggestion that they could represent useful index fossils for the Anthropocene (Hausdorf, 2018).

The shells of achatinid land snails consist of a $CaCO_3$ biomineral with an aragonitic crystal structure (de Paula and Silveira, 2009). In this study, shells of modern *Achatina tavaresiana* were observed to contain the same four-layered microstructure (Fig. 2) as those previously reported for *Lissachatina fulica* (Chaki et al., 1992). The microstructural layers, visible by scanning electron microscopy (SEM), include the periostracum (composed primarily of organic material and easily removed using a Dremel drill) and three aragonitic $CaCO_3$ layers (in this study termed '3AL': prismatic, cross-lamellar and nacreous).

The complex structures of achatinid shells, and indeed those of many other mollusc taxa (e.g. the bivalve genera *Mytilus* (Hare, 1963), *Arctica* (Haugen and Sejrup, 1990) and *Glycymeris* (Demarchi et al., 2015; Ortiz et al., 2017)), present two major challenges for AAG. The first is the possibility of microstructural protein differences: if different proteins control the architecture of the three aragonitic microstructural layers, then intra-specimen and/or inter-individual differences in the relative proportions of each layer would lead to variations in the relative abundance of these proteins. If these proteins break down at different rates due to differences in their peptide sequences (Smith and Evans, 1980; Mitterer and Kriausakul, 1984; Ortiz et al., 2013), the chronological signal obtained from protein diagenesis could become convoluted (Ortiz et al., 2013). The second challenge relates to mineral stability; aragonite is a metastable polymorph of calcium carbonate, which although kinetically stable can undergo conversion to the calcite polymorph over geological timescales (Brand and Morrison, 1987). Polymorphic conversion can lead to any originally entrapped amino acids not adhering to closed-system behaviour and becoming compromised during rearrangement (opening and subsequent closing) of the crystal structure (Penkman et al., 2007, 2010). To assess the potential impact of these issues, this study analysed samples taken from a single layer (nacreous) and from across all three aragonitic layers ('3AL': prismatic, cross-lamellar and nacreous; Fig. 2). The nacreous layer was selected due to sampling practicalities. Being the innermost layer, it was the easiest to obtain, with reliable sampling of the cross-lamellar and prismatic layers rendered impractical due to the overall thinness of the shell (~250 µm, Fig. 2).

One AAG approach shown to improve the reliability of the data in some mollusc shells is intra-crystalline protein degradation (IcPD) analysis. This approach targets protein trapped within the crystal matrix of biominerals, which may be isolated with a strong chemical oxidant (Sykes et al., 1995). This intra-crystalline protein fraction has been shown to operate as a closed system in many biominerals (e.g. gastropods (Penkman et al., 2008; Demarchi et al., 2013a), ostrich eggshell (Crisp et al., 2013), coral (Hendy et al., 2012), tooth enamel (Dickinson et al., 2019) and the calcareous tests of foraminifera (Millman et al., 2022)), and where this is the case, leaching of endogenous protein, contamination by exogenous protein and additional environmental impacts on protein degradation are minimised (Smith et al., 1978; Towe, 1980). In some biominerals, the IcPD approach to AAG has been shown to improve both the accuracy and precision of the data, increasing the reliability and robustness of the geochronologies obtained (e.g. Sykes et al., 1995; Penkman et al., 2008; Bosch et al., 2015; Ortiz et al., 2015). Oxidative treatment however is not always appropriate or necessary and, in these cases, stringent data screening approaches have also been used successfully for many AAG studies (e.g. Kaufman, 2006; Kosnik et al., 2008; Ortiz et al., 2018).

In this study we therefore evaluate the suitability of different shell layers in Achatininae shell for AAG using IcPD analysis, and consider its potential to build amino acid geochronologies across Africa in the future. We assess two sampling strategies (single-layer vs multi-layer) and investigate mineral stability by XRD analysis (section 3.1.3.). We investigate whether an intra-crystalline fraction of protein is present via bleaching experiments (section 3.1.1.), and whether this fraction

Table 1
Modern *Achatina tavaresiana* samples obtained from the Natural History Museum (NHM), London, and fossil *Lissachatina* sp. samples now archived in Livingstone Museum, Zambia, analysed in this study.

Sample ID	Museum registration number	Locality	Specimen type
PK.S19.3	ZM.LV.AR.9887	Site 19, Palaeolake Kafue	fossil
PK.S19.4	ZM.LV.AR.9888	Site 19, Palaeolake Kafue	fossil
PK.S19.20.1	ZM.LV.AR.9889	Site 19, Palaeolake Kafue	fossil
PK.S19.44	ZM.LV.AR.9890	Site 19, Palaeolake Kafue	fossil
PK.S19.45	ZM.LV.AR.9891	Site 19, Palaeolake Kafue	fossil
PK.S19.47	ZM.LV.AR.9892	Site 19, Palaeolake Kafue	fossil
PK.S19.48	ZM.LV.AR.9893	Site 19, Palaeolake Kafue	fossil
MA.NHM. UG.1	NHMUK20230327	Uganda	modern
MA.NHM. SC.1	NHMUK20230328	Seychelles	modern
MA.NHM. SC.1	NHMUK20230329	Mauritius	modern
MA.NHM. SC.1	NHMUK20230330	Tanzania	modern

behaves as a closed system through analysis of IcPD in forced degradation experiments on modern shells, and within fossils of Middle Pleistocene age (section 3.1.2.). Finally, we evaluate the ability of these elevated temperature experiments to mimic the protein degradation observed in Achatininae fossils, and therefore whether it is possible to use kinetic parameters derived from high temperature experiments to estimate age or burial temperature in Achatininae (section 3.2., SI section 4.).

2. Materials & methods

2.1. Materials

In this study four modern and seven fossil specimens were sampled (Table 1). In the absence of a universally accepted definition of the term "fossil", here we use the term to refer to preserved shell material within sediment. The modern specimens, obtained from historical collections in the Natural History Museum, London (NHM), all represent the West African species *Achatina taveresiana* Morelet, 1866. No record was made about how these specimens were collected, but the usual practice for high quality museum specimens is live collection and their pristine condition suggests this was the case. This species was chosen because shells identified as *A. tavaresiana* had previously been recorded from the Palaeolake Kafue (formerly known as Palaeolake Patrick) sequence (Simms, 2000). The fossils included in this study originated from sediments associated with Palaeolake Kafue (Site 19 chalky limestone (Fig. 3B), described in detail in SI section 1.), close to the Twin Rivers archaeological site in Zambia. The internal stratigraphic position of the molluscs within the chalky limestone was not recorded, although those recovered *in situ* were all from about the top 30 cm of the deposit. The fossil Achatininae shells studied here are therefore considered as a single time-equivalent population, although they may span a considerable time window.

The age of these lacustrine limestones is poorly constrained, but some inferences can be made from radiometric dates recovered from two nearby sites: the Twin Rivers kopje and the Casavera Stream, both on the

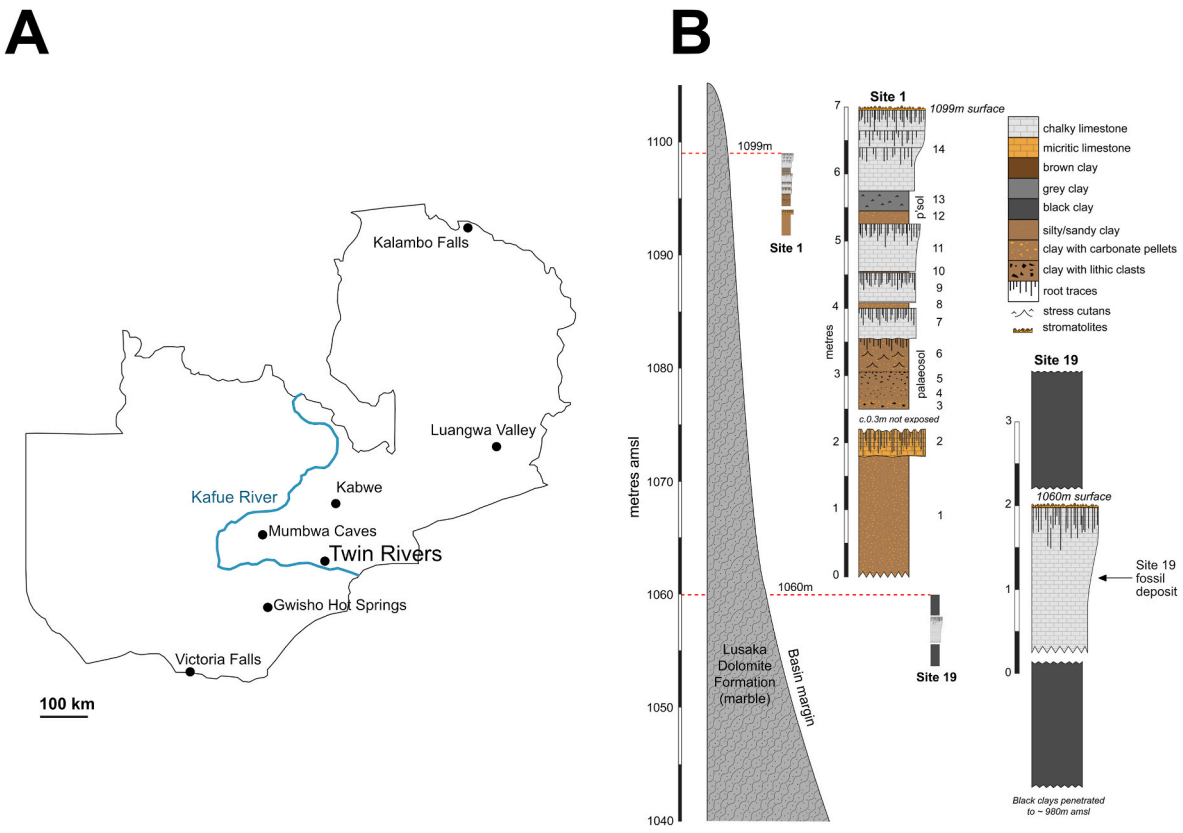

Fig. 3. A - Map of Zambia highlighting key archaeological sites and the modern Kafue River course. B – Stratigraphic sections showing the relationship between two relevant Palaeolake Kafue sites: Site 1, and Site 19. The fossils analysed in this study came from a single chalky limestone stratigraphic section (arrowed) within Site 19. Site 19 (S15°33′21.1″, E28°02′50.1″, altitude 1060 m amsl) is associated with Palaeolake Kafue, close to Twin Rivers archaeological site (S15°31, E28°11).

Table 2
Elevated temperature experiment conditions for the 3AL and 'nacreous' portions of modern *Achatina* shell. Due to sample constraints, only the two starred heating times at 140 °C were undertaken for *Achatina* 'nacreous'.

Temperature (°C)	Heating time (days)																
60	–	–	–	–	–	–	–	–	–	50	90	150	–	240	365	417	548
70	–	–	–	–	–	–	20	–	–	50	–	150	–	240	365	–	548
80	–	–	–	–	–	10	20	30	–	50	90	150	200	240	365	–	548
110	–	1	–	–	5	10	20	30	40	50	–	–	–	–	–	–	–
140	0.08	1*	2	3*	–	–	–	–	–	–	–	–	–	–	–	–	–

margins of Palaeolake Kafue. Various uranium-series (U-series) dates from Twin Rivers were obtained from calcite speleothem layers, ranging from >400 ka to ~140 ka. Two other U-series dates have been published for the Casavera stream 'fossil' tufa deposits (near Site 1, Fig. 3B) and these have an age range of ~200–400 ka (Barham et al., 2000: 179). An in-depth discussion of contextual information about the palaeolake and its dating is provided in the SI (section 1.). While it is not currently possible to further constrain the Site 19 sediments in age, from all the available information they are assumed to be Middle Pleistocene.

Because of significant restrictions on in-person research and access to museum collections caused by the COVID-19 pandemic in 2020 and 2021, formal identification of the fossil specimens was only possible after the laboratory experiments had been carried out. The fossils were identified as *Lissachatina* sp. based on the known biogeography of Achatininae, although the worn condition of the fossils and difficulty in using shell character to identify achatinids prevented species-level identification (Mead, 1991). Specimens previously identified as *A. tavaresiana* from the Palaeolake Kafue sequences (Simms, 2000) were examined, but the surviving specimens were either small fragments of shell or internal casts that could not be identified to species level. Given the known distributions of *Achatina* and *Lissachatina*, their previous identification as *A. tavaresiana* is unlikely to be correct. Regardless, the species represented are assumed to be sufficiently closely related within the subfamily Achatininae for comparative IcPD analysis.

Modern ostrich eggshell (OES) and shells of the terrestrial gastropod *Cepaea* sp. were used as calcite and aragonite $CaCO_3$ XRD reference material respectively (Feng et al., 2001; Kowalewska-Groszkowska et al., 2018).

2.2. Fossil cleaning

All fossil Achatininae shells excavated from Site 19 were filled with solidified sediment. The shells were soaked in water and where possible, the sediment manually removed.

2.3. Sampling

In order to identify an optimal sampling strategy, all shells in this study (four modern (for bleaching and elevated temperature experiments) and seven fossil specimens) were sampled for both their nacreous and three aragonitic layer (3AL) shell portions (Table 1). Shell periostracum was removed with an abrasive rotary burr on a handheld rotary tool (Dremel drill). The shell was washed and sonicated in water (ultrapure, 18.2 MΩ cm^{-1}) to remove any remaining powder before being air-dried. All specimens were sampled on the outermost whorl of each shell. Two shell portions were sampled from separate areas of this outermost whorl: the three aragonitic layers (3AL; comprising the prismatic, cross-lamellar and nacreous layers) and the nacreous layer. The 3AL portion was finely powdered with an agate pestle and mortar. The nacreous was removed from a separate area of each shell with an abrasive rotary burr on a handheld rotary tool (Dremel drill) and collected as a very fine powder. A cautious approach to removal of the nacreous was undertaken, but, since the microstructural layers were difficult to view both by eye and under standard laboratory microscope magnification, it is therefore possible non-nacreous layers were also incorporated. For this reason, this shell portion is termed the 'nacreous'. Whilst particle size has been shown to affect the variability of data obtained for coarse particles (500–1000 μm) in some shell species (e.g. *Patella*, Demarchi et al., 2013a), Penkman et al. (2008) found that particle size was shown not to affect the final concentration of amino acids, the rate at which the intra-crystalline fraction was reached, or the data variability for shells of the bivalves *Corbicula* and *Margaritifera* or the gastropod *Bithynia*. As a fine powder (<500 μm by eye) was collected for both the 3AL and 'nacreous' shell portions, no sieving was undertaken, in order to minimise the risk of loss of valuable material which occurs during the sieving process.

2.4. Isolation of the intra-crystalline protein fraction

To test whether an intra-crystalline fraction of protein was present within modern *A. tavaresiana* shell, bleaching experiments were undertaken following adapted methods of Sykes et al. (1995) and Penkman et al. (2008). Bleach (a strong chemical oxidant - 12% NaOCl (Fisher Scientific, analytical grade), 50 μL/mg) was added to *ca.* 20 mg of powdered sample (in separate 2 mL plastic microcentrifuge tubes (Eppendorf)) and left on a rotor (constant, mild agitation) for 24, 48 and 72 h, to test the impacts of bleaching time. The bleach was removed by pipette and each sample was washed five times with water (ultrapure, 18.2 MΩ cm^{-1}), before a final wash with methanol (Sigma-Aldrich, HPLC-grade) and left to air dry. Given the results presented in section 3.1.1., for all subsequent elevated temperature and fossil IcPD analysis, an optimised bleaching time of 48 h was used.

2.5. Elevated temperature experiments

Elevated temperature experiments on modern biominerals have routinely been used to investigate protein degradation on an accelerated timescale for comparative analysis to the geological diagenesis observed in fossils (e.g., Bada and Schroeder, 1972; Kimber and Griffin, 1987; Canoira et al., 2003; Penkman et al., 2008; Demarchi et al., 2013a; Tomiak et al., 2013; Ortiz et al., 2017; Dickinson et al., 2019). Following powdering (section 2.3.) and bleaching (section 2.4.), approximately 10 mg of modern shell was suspended in 300 μL water (ultrapure, 18.2 MΩ cm^{-1}) and isothermally heated for the times and temperatures given in Table 2. These samples were undertaken in experimental triplicate. 300 μL of water was used to enable comparative analysis to previous studies (e.g., Penkman et al., 2008; Demarchi et al., 2013a; Tomiak et al., 2013; Crisp et al., 2013) and the conditions are assumed not to affect the intra-crystalline fraction of protein, where closed-system behaviour has been adhered to. The water was removed by pipette and the samples were left to air dry prior to preparation for analysis (section 2.6.).

2.6. Amino acid analysis

Following the methods of Penkman et al. (2008), *ca.* 5 mg (accurate masses recorded) subsamples were weighed out for analysis of the free amino acid fraction (FAA) and the total hydrolysable amino acid fraction (THAA). FAA subsamples were demineralised in 2 M HCl (minimum possible volume) and dried in a centrifugal evaporator (*ca.* 24 h). THAA subsamples were demineralised in 7 M HCl (20 μL/mg), the vials flushed

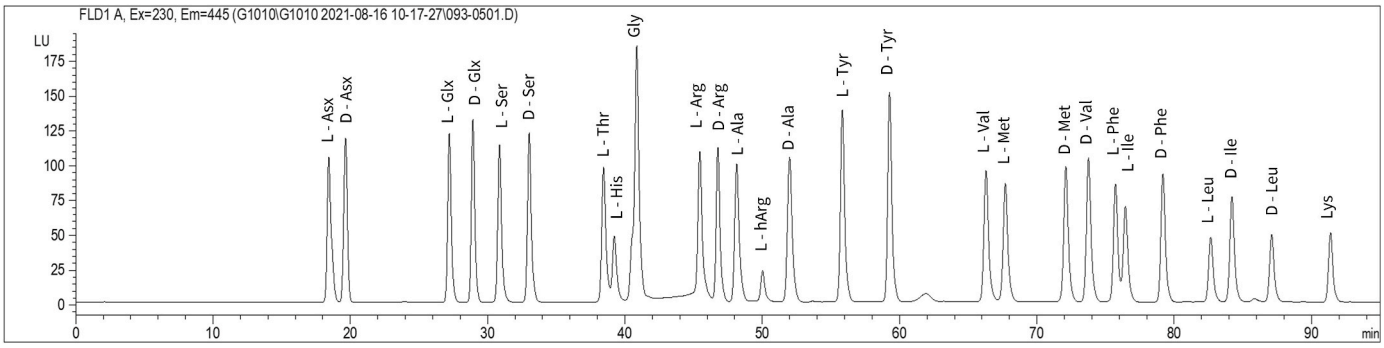

Fig. 4. Example chromatogram of a standard.

with N_2 and heated to 110 °C for 24 h, prior to drying in a centrifugal evaporator (*ca.* 24 h). All subsamples were rehydrated (10 μL/mg) in a solution of internal standard (L-homo-arginine, 0.01 M), hydrochloric acid (0.01 M) and sodium azide (1.5 mM). Separation of the chiral isomers of the amino acids was carried out by fluorescence detection reverse phase high performance liquid chromatography (RP-HPLC; Fig. 4) using a modified Kaufman and Manley (1998) method (Penkman, 2005). As experimental replicates were prepared, no analytical replicates were undertaken; analytical replicates have been shown to account for only a small portion of the total variability, hence the use of subsample experimental replicates also encompasses analytical variability (Powell et al., 2013).

Total amino acid concentration and relative composition calculations were carried out for Asx, Glx, Ser, L-Thr, L-His, Gly, Arg, Ala, Tyr, Val, Met, Phe, Ile and Leu. In the case of Thr and His only the L enantiomer is resolved by this chromatographic method, whilst Gly contains no stereogenic centre and therefore does not have L/D enantiomers (Fig. 4). Sufficient concentration and chromatographic resolution were achieved for the calculation of racemisation and percentage free values for Asx, Glx, Ser, Ala, Val, Phe within the achatinid shells (see SI data).

2.7. Assessment of mineral diagenesis

Crystal structure polymorphism was analysed by X-ray diffraction (XRD) analysis. This was to test for mineral diagenesis, specifically the conversion of aragonite, the metastable polymorph of $CaCO_3$, to calcite, as mineral diagenesis can result in the targeted intra-crystalline protein becoming compromised from rearrangement (opening and subsequent closing) of the crystal structure (Preece and Penkman, 2005; Penkman et al., 2010). Analysis was undertaken on two instruments (due to availability at time of analysis of the samples). Approximately 10 mg of powdered sample was flattened onto a specimen holder (Malvern or Bruker silicon single crystal low background specimen folder for small specimen amounts) with a glass microscope slide. XRD analysis was carried out using two methods adapted from Lesbani et al. (2013). On the Panalytical Aeris diffractometer, each sample was scanned between 5 and 70° 2θ at a scanning speed of 0.2° s^{-1}; on the Bruker D8 diffractometer, each sample was scanned between 0 and 120° 2θ using a 0.05° increment with a measurement time of 0.1 s per step.

3. Results & discussion

3.1. Assessment of suitability for IcPD analysis

3.1.1. Assessment of intra-crystalline protein fraction - bleaching experiments

Bleaching experiments were undertaken to first assess whether an intra-crystalline fraction of protein was present within Achatininae shell, and if so, to determine the optimal exposure time. The concentration of all hydrolysable amino acids decreased within both the 3AL shell portion and the 'nacreous' layer of *A. tavaresiana* shell post-exposure to bleach (Fig. 5, SI Fig. 1). No appreciable difference in concentration was observed between the bleach times investigated. The stable concentrations of amino acids remaining post-bleaching are therefore hypothesised to be the protected intra-crystalline fraction (Sykes et al., 1995), with the unbleached samples also containing an inter-crystalline fraction that is exposed to the environment.

No significant differences in protein composition were observed between the unbleached and any of the bleached (24, 48 and 72 h) 3AL shell samples (Fig. 6A). It is therefore likely that the inter- and intra-crystalline protein fractions contain similar protein compositions and have minimal contamination in these samples. There was, however, a

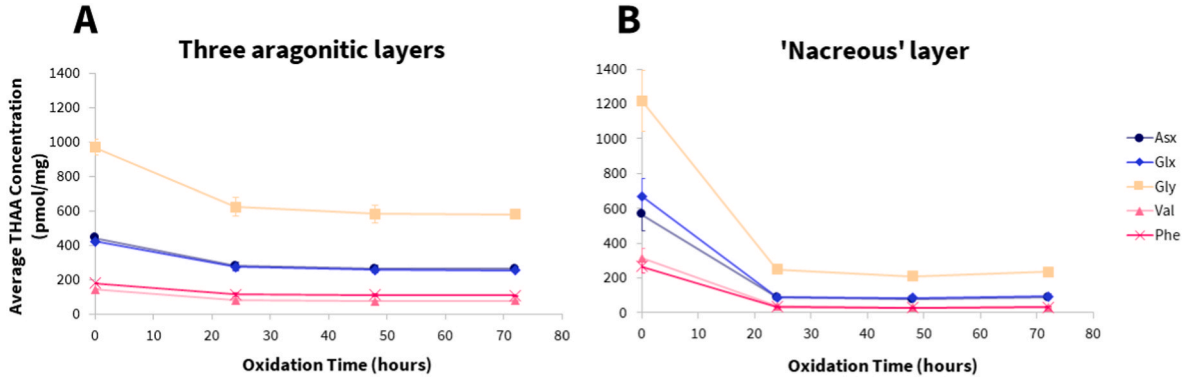

Fig. 5. Average THAA concentration for five example amino acids in modern *Achatina tavaresiana* shell portions (A - 3AL, B - 'nacreous' layer); powdered shell was analysed unbleached (0 h) and exposed to NaOCl, a strong chemical oxidant, for 24, 48 and 72 h. Error bars represent the standard deviation about the mean for subsample experimental triplicates. Within 24 h a decreased, stable concentration of amino acids was achieved in both shell portions, defined as the intra-crystalline protein fraction.

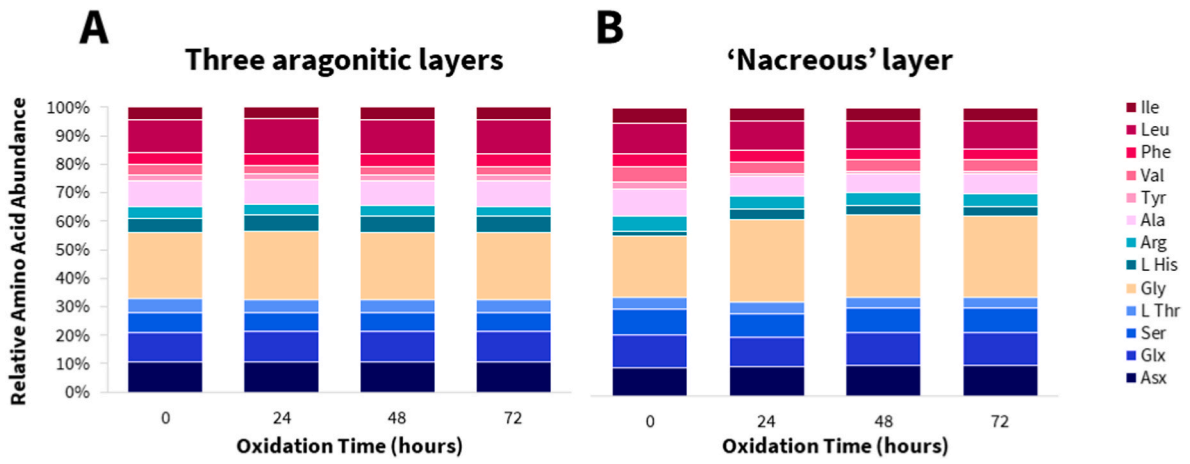

Fig. 6. Relative amino acid composition of the THAA fraction in modern *Achatina tavaresiana* shell portions (A - 3AL, B - 'nacreous' layer) after the shell was exposed to NaOCl, a strong chemical oxidant, for 0, 24, 48 and 72 h.

difference in composition upon bleaching for the 'nacreous' samples (Fig. 6B). This could be due to different proteins within the inter- and intra-crystalline fractions, and/or as a result of the sampling method of obtaining Achatininae 'nacreous'. As the 'nacreous' is drilled off the shell as a powder (unlike 3AL shell sampling which uses a pestle and mortar), contamination from proteins within the cross-lamellar layer is possible. Nonetheless, it is worth noting that minimal differences were observed between the samples which were bleached for 24, 48 and 72 h (Fig. 6B), indicating the bleach successfully removed any contamination and the inter-crystalline protein from the 'nacreous' sample.

As far as we are aware, no studies have been undertaken to characterise the proteins in the individual microstructural layers of achatinid shell. The differences in relative amino acid abundance between 3AL shell portion and 'nacreous' (Fig. 6, e.g. Gly 24% ± 1% in the 3AL and 29% ± 1% in the 'nacreous', for all samples exposed to bleach) therefore suggest a difference in protein composition between the two shell portions.

The bleaching experiments therefore indicate that an intra-crystalline fraction of protein is present within Achatininae shell, which was successfully isolated by exposure to NaOCl, a strong chemical oxidant. For all subsequent experiments and analyses, a bleaching time of 48 h was chosen, consistent with methodologies of other shell material (Penkman et al., 2008; Demarchi et al., 2013a).

3.1.2. Assessment of closed system behaviour

After establishing that Achatininae shell has an intra-crystalline fraction of protein present within the 'nacreous' and 3AL shell portions (section 3.1.1.), we then assessed whether degradation within this fraction was consistent with closed-system behaviour.

3.1.2.1. Elevated temperature kinetic experiments – racemisation and hydrolysis. Elevated temperature kinetic experiments are used to investigate protein degradation on an accelerated timescale for comparison with the diagenesis observed in fossils (e.g., Bada, 1972; Kriausakul and Mitterer, 1978; Kimber and Griffin, 1987; Canoira et al., 2003; Kaufman, 2006; Clarke and Murray-Wallace, 2006), and can also be used to test closed-system behaviour of any intra-crystalline protein fraction (Penkman et al., 2008; Hendy et al., 2012; Demarchi et al., 2013a; Dickinson et al., 2019). In achatinid shell, it is likely that different proteins are contained within the different aragonitic layers (prismatic, cross-lamellar and nacreous) as a result of having controlled the distinct $CaCO_3$ architecture (section 3.1.1.). The peptide sequence, unique to each protein, influences protein degradation and rates of amino acid racemisation (Smith and Evans, 1980; Mitterer and Kriausakul, 1984; Ortiz et al., 2013). As sampling was undertaken on both the 3AL shell portion and the 'nacreous' layer, elevated temperature experiments can therefore also be used to investigate the protein degradation within different microstructural shell portions.

As expected for protein degradation, at each elevated temperature the extent of racemisation increased with time for all amino acids (Figs. 7 and 8, SI Figs. 2 and 3). In general, greater variability in the

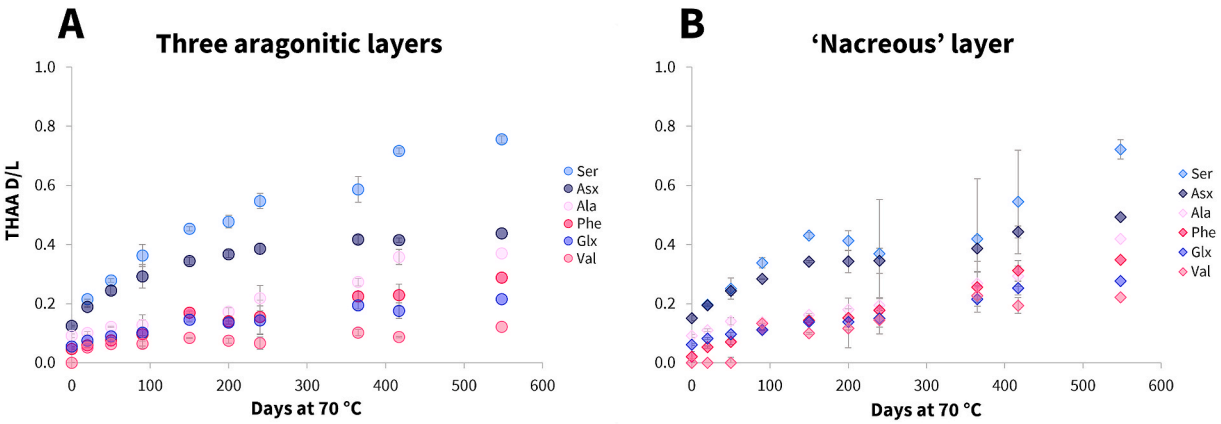

Fig. 7. The extent of racemisation for the hydrolysable amino acids in the 3AL shell portion (A) and the 'nacreous' layer (B) of modern *Achatina tavaresiana* shell, during isothermal heating at 70 °C. Error bars represent the standard deviation about the mean for subsample experimental triplicates. An increase in racemisation was observed for all amino acids, at different relative rates.

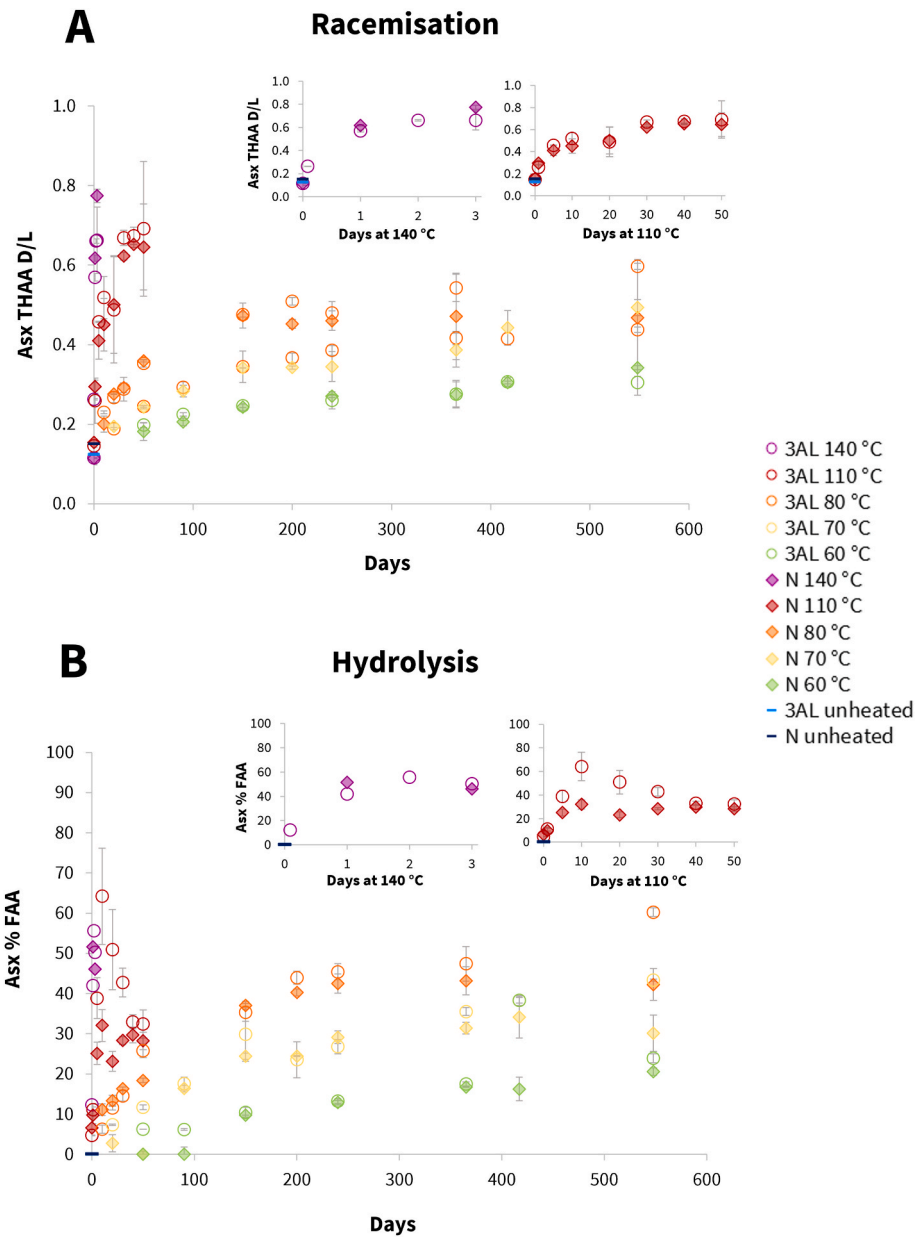

Fig. 8. The extent of racemisation (A) and peptide chain hydrolysis (B) in Asx in bleached modern *Achatina tavaresiana* shell during isothermal heating at 60, 70, 80, 110 & 140 °C. Error bars represent the standard deviation about the mean for subsample experimental triplicates. An increase in racemisation and hydrolysis was observed for Asx with respect to both time and temperature.

extent of racemisation (D/L) was observed for amino acids in the 'nacreous' layer in comparison to the 3AL shell portion (e.g., Fig. 7). This may be a sampling issue (section 3.1.4.) or because the 'nacreous' intracrystalline protein fraction doesn't operate as a closed system (Ortiz et al., 2017; Wheeler et al., 2021). For the majority of the temperatures (Fig. 7, SI Fig. 2), similar trends for both the 3AL and 'nacreous' layer were observed to the reported relative racemisation rates for free amino acids (Asp > Phe > Ala > Glu > Val; Smith and Evans, 1980). In proteins, with the exception of Ser and Asx (Demarchi et al., 2013b), the majority of amino acids are not able to freely racemise in chain, requiring greater conformational freedom (terminal or free) to do so. Any differences in the relative rates of racemisation here (in comparison to free amino acids) are likely as a result of additional influential factors for proteins within biominerals, such as the peptide sequence and biomineral interactions (e.g., Demarchi et al., 2016).

Additionally, as expected the extent of racemisation (D/L) increased for all amino acids with increasing temperature (e.g., Asx in Fig. 8A, SI Fig. 3). Similar patterns of degradation were also observed for peptide chain hydrolysis (e.g., Asx in Fig. 8B, SI Fig. 4). Interestingly, at 70 °C and 80 °C, Asx in the 3AL appeared to hydrolyse much faster than in the 'nacreous' layer (Fig. 8B). At 110 °C, Asx in the 3AL also showed a different hydrolysis pattern to the 'nacreous' layer (Fig. 8B). These temperature-related differences were also observed for the other amino acids studied (Glx, Ser, Ala, Val, Phe; SI Fig. 4). Differences between the 'nacreous' layer and 3AL peptide chain hydrolysis rates may be because of primary protein sequence differences (with respect to both the relative peptide bond strengths arising from different neighbouring amino acids in the peptide chain (Hill, 1965), and/or to different mineral surface interactions and solvent (water) effects (Demarchi et al., 2016)).

3.1.2.2. FAA vs THAA in artificially degraded shells and fossils. From IcPD analysis, closed-system behaviour can be inferred in several ways including from a strong positive correlation between the FAA and THAA extent of racemisation (Penkman et al., 2008). In general, the 3AL

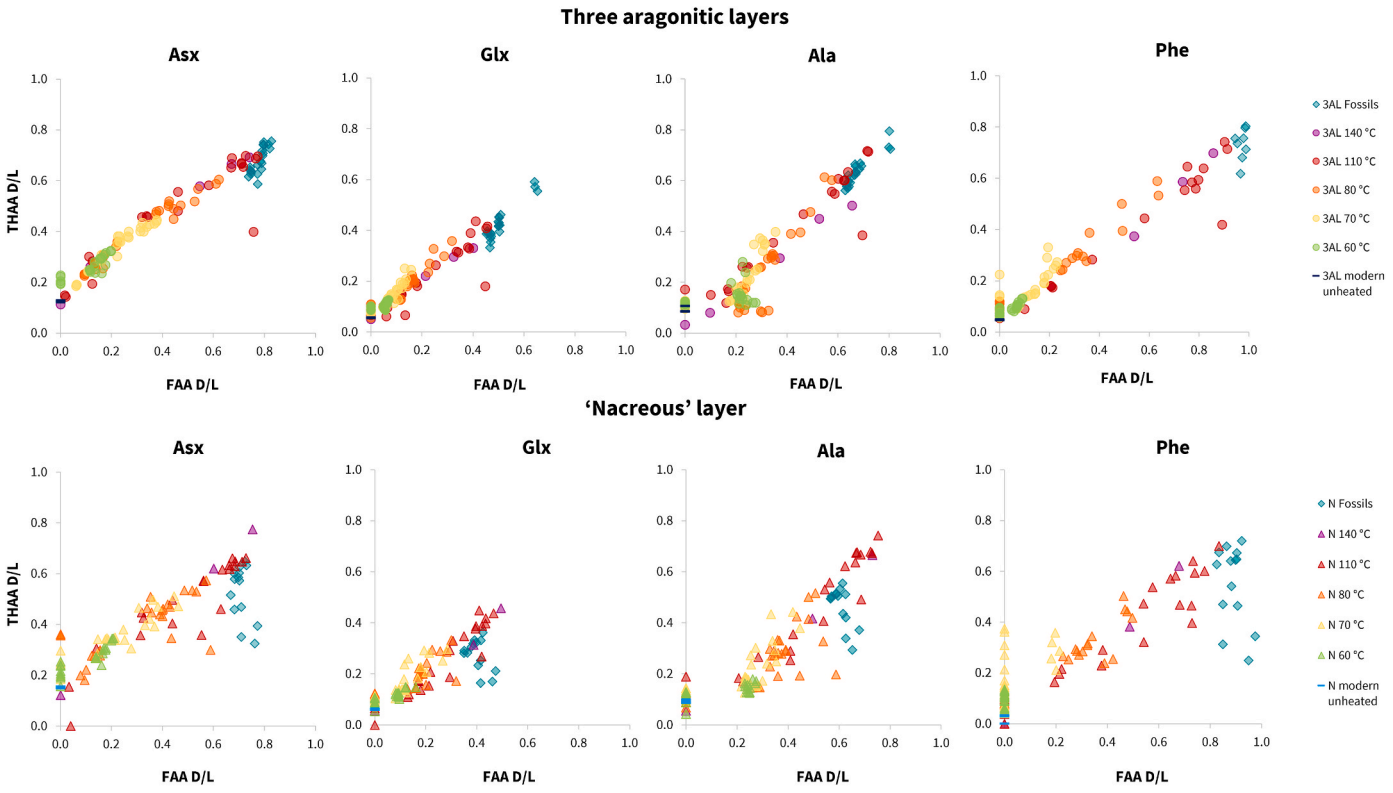

Fig. 9. Intra-crystalline free amino acid (FAA) vs total hydrolysable amino acid (THAA) racemisation values (D/L) for four amino acids (Asx, Glx, Ala, Phe) from elevated temperature experiments on modern *Achatina tavaresiana* shell unheated and at 60, 70, 80, 110, and 140 °C, and from *Lissachatina* sp. fossils. Upper: 3AL; lower: 'nacreous' layer. For any data points plotted at 0 (on the x and/or y axis), the concentration of the D isomer was below the limit of detection.

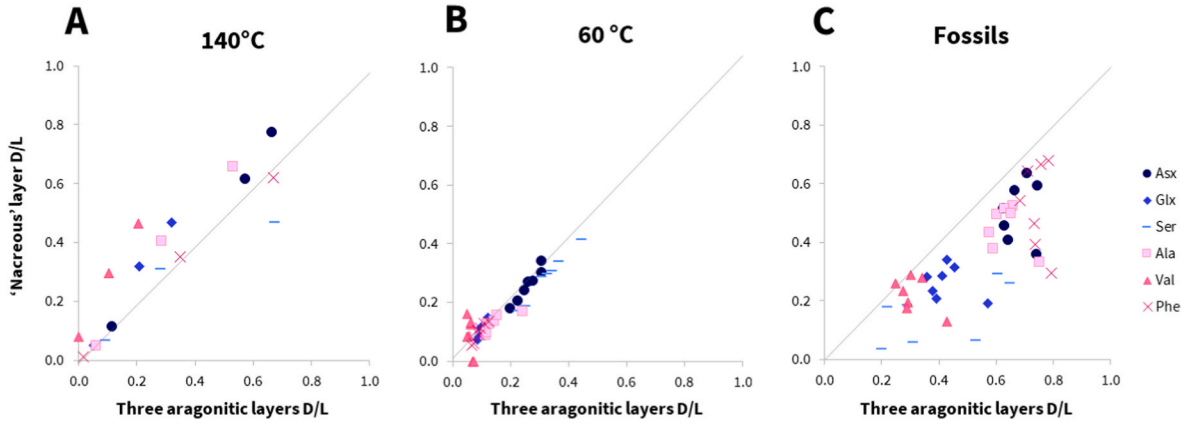

Fig. 10. Comparison between the mean extent of racemisation for total hydrolysable amino acids (THAA) of modern *Achatina tavaresiana* shell during elevated temperature experiments at 140 °C (A) and 60 °C (B) and *Lissachatina* sp. fossils (C). The central grey line marks a theoretical 1:1 ratio; for data above this, amino acids are racemising quicker in the 'nacreous' layer; below, those in the 3AL are faster. Importantly this relationship changes between the high temperature experiments and fossil samples at lower burial temperatures.

displayed a stronger positive correlation between D/L values in the free and hydrolysable amino acid fractions for the majority of amino acids (four best chromatographically separated amino acids given in Fig. 9), in both modern heated and fossil samples. Greater variability in the extent of racemisation was observed in the 'nacreous', especially within the THAA for both the modern heated and fossil samples (Fig. 9), indicating either inconsistent sampling or poorer adherence to closed-system behaviour (discussed in detail below in sections 3.1.3-4).

A range of relatively high racemisation values were obtained for the fossil *Lissachatina* sp. samples (Fig. 9), either because they represent a range of ages within the Middle Pleistocene (consistent with section 2.1. and SI section 1.) and/or resulting from the fossils having experienced different temperature histories. The latter may occur for fossils of similar age which have experienced different integrated burial temperatures (Wehmiller et al., 2000) or through heating events such as cooking (Wojcieszak et al., 2023). Consideration of temperature histories is therefore an important factor for future studies where relative chronologies, which rely on the extent of racemisation as a marker for regional time, are being built. However, as these fossil samples are used to represent naturally aged samples (rather than being of known specific ages), their data is useful here for making comparisons to experimentally degraded material.

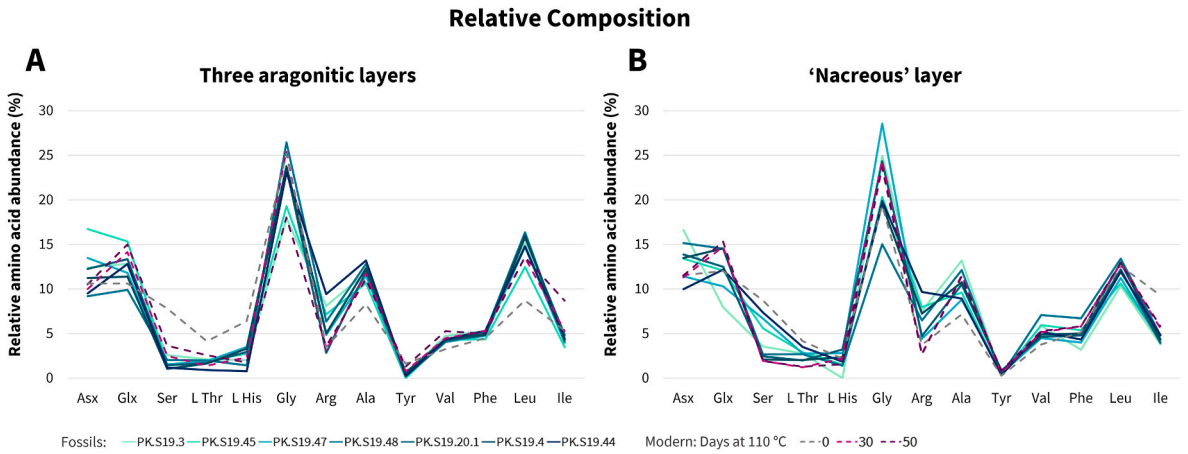

Fig. 11. Comparison of the mean relative amino acid abundances for the total hydrolysable amino acids (THAA) in the 3AL (A) and 'nacreous' (B) shell portions of the *Lissachatina* sp. fossil samples and *Achatina tavaresiana* modern unheated samples with similar extents of Glx racemisation from heating to 110 °C. The fossil samples have been colour-coded in order of increasing extent of Glx racemisation from the 3AL shell portion (darker teal = higher Glx D/L).

3.1.2.3. Shell microstructural layer differences in artificially degraded and fossils. During elevated temperature experiments, the majority of amino acids from both the 3AL and 'nacreous' layer racemised at a similar relative rate between 60 °C (Fig. 10B) — 110 °C. One exception was observed, valine, which racemised more quickly in the 'nacreous' layer at every temperature (e.g., Fig. 10A and B). At 140 °C, systematic differences in the extent of relative racemisation were observed between the 3AL and 'nacreous' layer for a number of amino acids (Fig. 10A). The naturally degraded fossils showed a different trend to the elevated temperature experiments, contrary to the 140 °C data, with the majority of amino acids more highly racemised in the 3AL shell portion than in the nacreous layer (Fig. 10C). There are a few possible reasons for this. One explanation is that the conditions used for the accelerated degradation experiments (powdered, bleached shell in water) don't reflect the environmental degradation conditions experienced by shells (here from Site 19 chalky limestone, Fig. 3B), and therefore the degradation mechanisms may be influenced by these environmental differences. However, this would not be the case if the intra-crystalline fraction of protein within achatinid shell truly displayed closed-system behaviour, as theoretically all external influences except temperature are removed. Another explanation for the divergent relative racemisation rates at different temperatures is that different protein degradation mechanisms may be occurring at high temperatures compared to those experienced by the fossils at lower environmental temperatures; this has been observed before in other biominerals (e.g. coral (Tomiak et al., 2013) and the marine bivalve *Pecten* (Pierini et al., 2016)).

For the 3AL, the relative amino acid compositions of the fossil shells were largely comparable to those with similar extents of Glx racemisation from the heating experiments and dissimilar to the modern, unheated sample (Fig. 11A). These include markers of protein degradation such as the decomposition of Ser to Ala (Bada et al., 1978), with lower %Ser and higher %Ala for increasingly degraded samples (SI Fig. 6). The total amino acid concentrations observed in the fossils were in general lower than those observed in the modern heated samples, but not dissimilar to the concentrations observed in those heated to 60, 70 and 80 °C for the longer time periods (SI Fig. 5). This further indicates that the intra-crystalline fraction of the 3AL shell portion behaves as a closed system. The concentration (SI Fig. 5) and relative composition of the 'nacreous' layer shell portion (Fig. 11B) was more variable between fossils; when considered in combination with the wider spread of racemisation values observed (Fig. 9), it is likely that the protein in this shell portion is a less reliable marker of time for building AAGs than the 3AL shell portion.

The apparent adherence to closed-system behaviour in the 3AL showcases the potential suitability of 3AL portion of Achatininae shell for future IcPD analysis to build regional AAGs across Africa.

3.1.3. Assessment of mineral diagenesis

XRD analysis was undertaken to assess the aragonitic $CaCO_3$ crystal structure of modern and fossil Achatininae (de Paula and Silveira, 2009). Whilst kinetically stable, aragonite may undergo conversion to the calcite polymorph over geological timescales (Brand and Morrison, 1987), potentially leading to the target intra-crystalline fraction of amino acids becoming compromised from rearrangement (opening and subsequent closing) of the crystal structure (Penkman et al., 2010). XRD analysis of the powdered (via drilling for 'nacreous' and pestle and mortar for the 3AL) fossil Achatininae shell samples resulted in diffractograms which largely matched the aragonitic reference, but with evidence of a weak calcitic diffraction peak from at ~ 29° 2Θ for a number of samples (Fig. 12).

Evidence for the presence of calcite in the fossil samples was very weakly observable in 2/7 3AL samples (e.g. PK.S19.3 W, Fig. 12) and in 4/7 'nacreous' samples (e.g. PK.S19.3 N and PK.S19.44 N, Fig. 12). This indicated that thermodynamic conversion of aragonite to calcite may have occurred in some of the fossil samples. There was however no clear relationship between the presence of calcite and the extent of subsample replicate variability. As only a portion of each fossil sample was analysed by XRD prior to IcPD analysis, it is not possible to say with certainty that where it was not observed, mineral diagenesis may not have occurred in another sampled part of the shell. Additionally, whether the presence of calcite resulted from mineral diagenesis during the fossils' burial history is difficult to assess, since evidence of calcite was also observed in modern Achatininae shell 'nacreous' (but not 3AL), both prior to and during elevated temperature experiments (Fig. 13). In the 'nacreous' this may be induced by the sampling process, due to the mechanical pressure and heat of drilling off the 'nacreous' from the inside of the shell (Foster

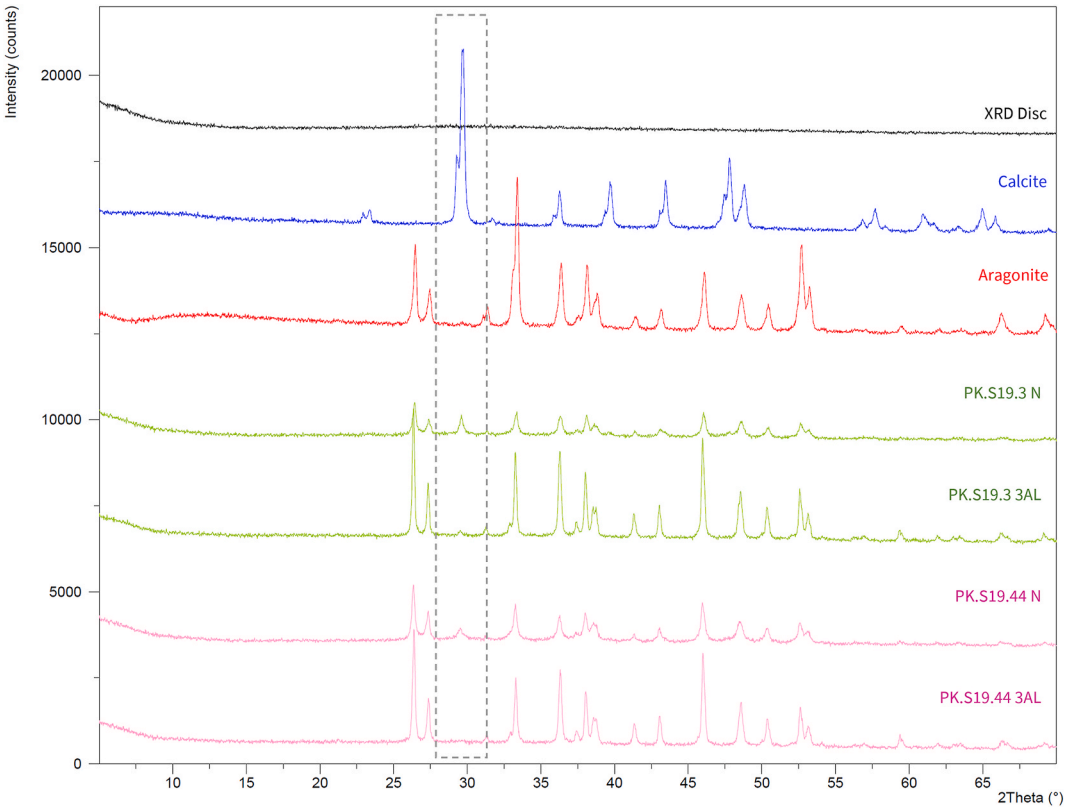

Fig. 12. Diffractograms of two fossil *Lissachatina* sp. shells, sampled from both the 3AL and 'nacreous' (N) of each shell in comparison to calcite and aragonite $CaCO_3$ references. The dashed box highlights the dominant calcitic diffraction peak at ~29° 2Θ; this shouldn't be present in an aragonitic sample but is present in both fossil 'nacreous' layers. Please note, the diffractograms have been offset on the y axis for visibility and the spectral counts left for relative scale.

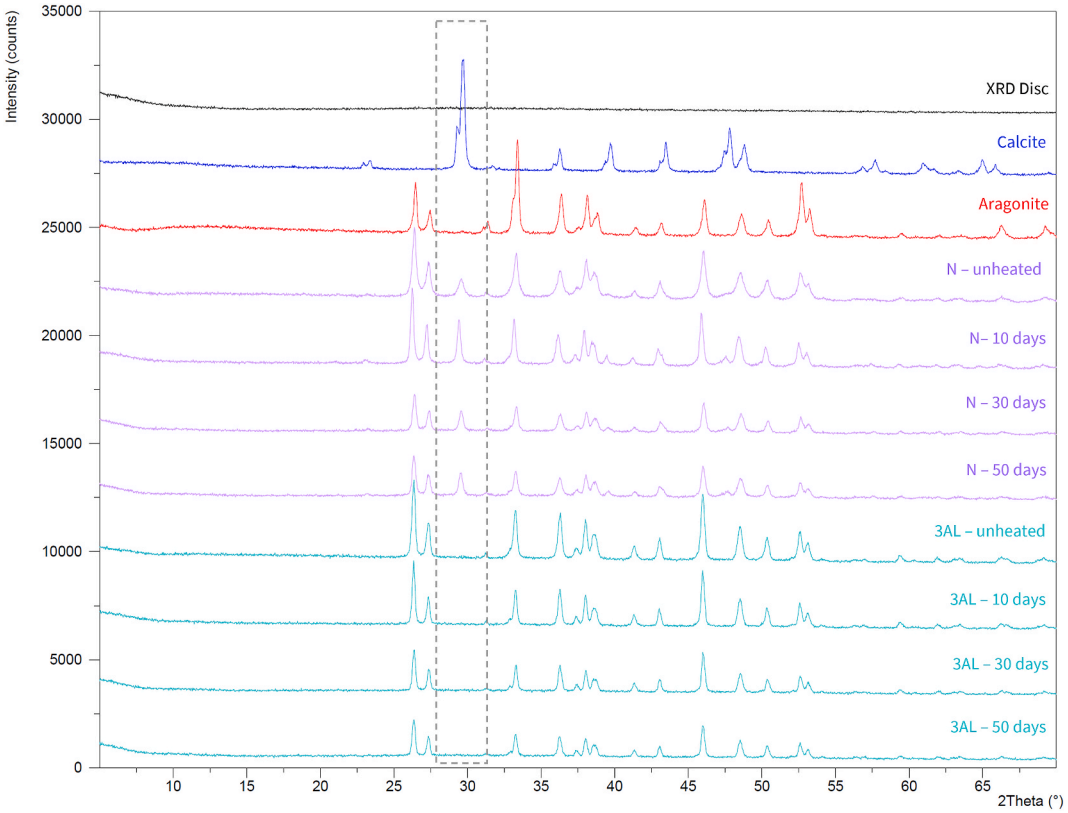

Fig. 13. Diffractograms of modern *Achatina tavaresiana* shell 3AL and 'nacreous' samples heated to 110 °C for 0, 10, 30 and 50 days. The dashed box highlights the dominant calcitic diffraction peak at ~29° 2Θ. The calcite peak was present in all nacreous samples, but not the 3AL samples. Please note, the diffractograms have been offset on the y axis for visibility and the spectral counts left for relative scale.

et al., 2008). Given this, we recommend that sampling by drilling is minimised wherever possible in this shell material to avoid induced remineralisation.

3.1.4. Sampling considerations and recommendations

Evidence that different proteins may be found in the 'nacreous' to other microstructural layers in achatinid shell was observed from the relative amino acid abundances in section 3.1.1. Whilst targeting a single layer, such as the nacreous, would theoretically be preferred in order to reduce the possibility of different proteins within different microstructural layers confusing the chronological signal, we do not recommend this sampling strategy for Achatininae shell for two reasons. Firstly, achatinid shell is ~250 μm thick (Fig. 2). Whilst the microstructural layers are clear under the magnification of a SEM (Fig. 2), distinguishing the boundary between the nacreous and cross-lamellar layers is rarely possible by eye. This results in the need to sample the nacreous very cautiously to minimise accidental sampling of the cross-lamellar layer. Taking this approach therefore requires much more shell to be sampled to obtain sufficient nacreous for analysis. Secondly, the mechanical pressure and heat from the rotary drill during sampling may give rise to thermodynamic conversion of aragonite to calcite (section 3.1.3.). If this occurs, it becomes difficult to assess the fossil's mineral diagenetic history (i.e., whether closed-system behaviour has been adhered to, and subsequently whether racemisation values are a reliable signal of endogenous protein degradation). Due to the potential size of achatinid shells, fossils may often be found incomplete, with only apices or body whorls present. Additionally, the fossils studied here contained solidified sediment which was challenging to remove. As it was beyond the scope of this study to investigate intra-specimen variability, we sampled all specimens on the outermost whorl of each shell. We therefore currently recommend that future studies sample only the 3AL shell portion from the outermost whorl, where consistent degradation patterns and closed-system behaviour was observed in both modern heated and fossil samples (3.1.2.), and for its relative ease of consistent sampling, known to reduce the potential for intra-shell variability (Murray-Wallace, 1995; Hearty and Kaufman, 2009).

3.2. Kinetic behaviour

Numerical age estimates can be calculated from fossil amino acid racemisation data through the application of mathematical models that use accelerated degradation experiments and/or calibration using additional dating techniques. Mathematical models have been used with mixed results (e.g., Tomiak et al., 2013 and references therein), but have been successfully employed for a number of biominerals (e.g., Clarke and Murray-Wallace, 2006; Wehmiller et al., 2012; Torres et al., 2014). In these cases, meaningful extrapolation has been possible where the high-temperature protein degradation experiments mimic the mechanisms occurring in naturally degraded fossils. The disparity between the 'nacreous' layer and 3AL relative racemisation patterns in section 3.1.3. provides potential evidence that this is not the case for achatinids. To explore this further, we investigated the predictions for fossil age and temperature made by two commonly used mathematical models (Clarke and Murray-Wallace, 2006). Data from our high temperature (60 – 140 °C) experiments were modelled using apparent reversible first order kinetics ($RFOK_a$) and constrained power law kinetics (CPK); see supplementary information (SI section 4) for a detailed description. Linearisation of the experimental data using these models was variable, with some amino acids achieving very high levels of linearity (e.g., Ala, Fig. 14B), whilst others had poor fit (e.g., Asx, Fig. 14A). This poor fit of Asx results from its rapid initial racemisation rate (likely due to its ability to racemise when bound in a peptide chain (Demarchi et al., 2013b)), and from the observed Asx signal being a combination of aspartic acid and asparagine, giving rise to a more complex 'observed' rate signal (e.g. Goodfriend et al., 1992).

In making the assumption that the reaction pathways are the same at all temperatures and undertaking accelerated degradation experiments at a minimum of three temperatures, it is possible to calculate the activation energy (E_a) for racemisation using the Arrhenius equation (SI equation 4). Activation energies were calculated for all amino acids where 'good' linearity ($R^2 > 0.97$ as suggested by Crisp et al. (2013)) was achieved through the mathematical transformations (Ala, Table 3 and Phe SI Table 1). In general, where very high levels of linearity ($R^2 > 0.995$) were observed, there was little difference in the resulting activation energies from $RFOK_a$ and CPK (e.g., Ala ~96 kJ mol^{-1} for both, Table 3). Interestingly a greater discrepancy was observed for the calculated activation energy for Ala racemisation in the 'nacreous' (96.8 kJ mol^{-1} using $RFOK_a$ vs. 119.0 kJ mol^{-1} using CPK), even though very high levels of linearity were observed for both kinetic models. Variability between activation energies calculated using different mathematical models has previously been reported (Crisp et al., 2013; Tomiak

Table 3
Activation energies of Ala racemisation calculated from the Arrhenius equation (SI equation 4) using data from five elevated temperature experiments (60, 70, 80, 110, 140 °C) on modern *Achatina tavaresiana* shell.

Amino acid	Shell fraction	Kinetic model	n	Model fit (R^2)	E_a (kJ mol^{-1})
Ala	3AL	$RFOK_a$	n/a	0.996	95.7
		CPK	1.2	0.998	97.5
	'Nacreous'	$RFOK_a$	n/a	0.988	96.8
		CPK	1.9	0.990	119.0

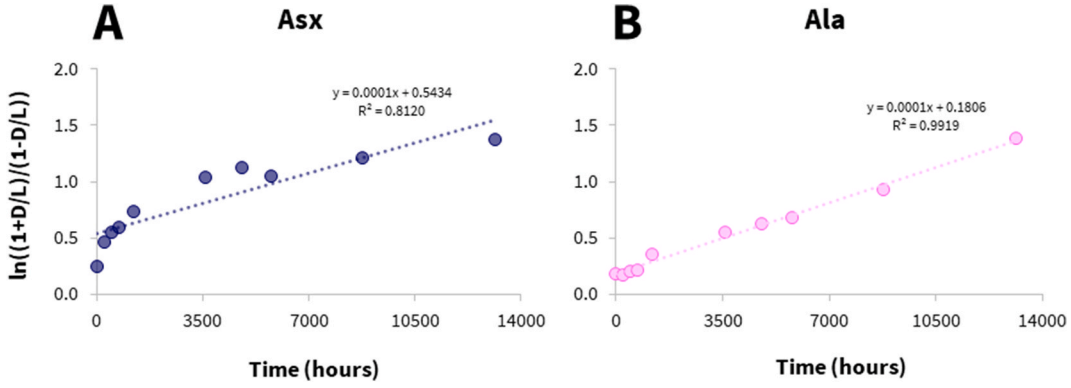

Fig. 14. Assessment of fit for the linearised relationship between the time spent at 80 °C and transformed THAA D/L values for Asx (A) and Ala (B) using RFOK (SI equation 2), for 3AL. The linearity of transformed D/L values was variable between amino acids, indicating $RFOK_a$ is not a suitable kinetic model to describe all amino acid racemisation within the intra-crystalline fraction of Achatininae shell.

Table 4
'Kinetic age' and 'kinetic temperature' calculations using two fossils from both their 3AL and 'nacreous' for Ala. 'Kinetic ages' were calculated using Lusaka, Zambia's current mean annual temperature (MAT, 20.4 °C). 'Kinetic temperatures' were calculated using arbitrary fossil ages of 200 ka and 400 ka for these Late Middle Pleistocene fossils. Note that the 'kinetic age' and 'kinetic temperature' outputs from the mathematical models do not agree with the palaeoenvironmental information for these fossils and should not be interpreted as accurate values for this site.

Fossil ID	Shell fraction	'Kinetic age' (years) using current MAT: 20.4 °C	'Kinetic temperature' (°C) using fossil age: 200 ka	'Kinetic temperature' (°C) using fossil age: 400 ka
PK. S19.44	3AL	2705	−8.6	−12.7
	'Nacreous'	1673	−9.1	−12.9
PK. S19.45	3AL	1724	−11.3	−15.4
	'Nacreous'	2468	−7.0	−10.8

et al., 2013; Dickinson et al., 2019), and this may be due to the validity of the mathematical transformations to each dataset, which encompasses issues due to different reaction pathways being made available at higher temperatures.

3.2.1. *Plausibility of predicted fossil ages and diagenetic temperatures*

To explore a best-case scenario, we used amino acids with good model fits (high R^2 values), to gauge whether these mathematical models could be used to calculate plausible numerical ages or past climate temperatures for the fossils based on their extent of racemisation. Although there is no direct evidence for the age of the shell material from Site 19, there is strong circumstantial evidence (discussed in section 2.1., SI section 1) that the sediments at Sites 1 and 19 are broadly coeval in age with the occupation of the Twin Rivers kopje and are probably Late Middle Pleistocene in age. Assigning an arbitrary date of 200 ka to two of the fossils (with the highest and lowest racemisation values) resulted in extrapolated integrated climate temperatures between −7.0 and −11.3 °C when using Ala (Table 4). If the samples are older (400 ka), then the extrapolated temperatures are even lower (from between −10.8 °C and −15.4 °C, depending on the model). Given this requires the site to be below freezing for its history, this is an incredibly unlikely range for the average integrated temperature of the sediment for Palaeolake Kafue, Zambia. Likewise, whilst Lusaka's current mean annual temperature (20.4 °C) would be an overestimation of the average regional temperature during the Pleistocene climate oscillations, the calculated ages using this temperature estimate are a factor of ten lower than their expected age and fall within the Holocene (Table 4).

The highly implausible results produced by the $RFOK_a$ and CPK models for the Achatininae shells studied here (Table 4, SI Table 1) may be due to protein decomposition pathways being different at lower environmental (burial) temperatures than they are under the high-temperature experiments in the intra-crystalline fraction of this biomineral (discussed in section 3.1.2.3.), as has been observed for some other biominerals (e.g. Tomiak et al., 2013). Whilst the assumption is that the intra-crystalline protein fraction is not influenced by any external factors other than temperature, in this case it is also possible that the conditions used for the accelerated degradation experiments (powdered, bleached shell in 300 μL water), were not a good proxy for naturally degraded shell samples. Experimental influences may therefore have rendered these samples inappropriate for extrapolation in this case. Nevertheless, the consistent patterns of racemisation in Achatininae (section 3.1.2.) mean this taxon still holds potential for building relative amino acid geochronologies across Africa in the future.

4. Conclusion

The shells of land snails in the subfamily Achatininae (modern *Achatina tavaresiana* and fossil *Lissachatina* sp.), which have complex multi-layered $CaCO_3$ shell microstructures, were assessed for their potential suitability for building amino acid geochronologies using IcPD analysis. Comparison was made between the three aragonitic layer (3AL) shell portion and the 'nacreous' layer alone in order to assess the most appropriate sampling strategy. Achatininae shell was shown to have an intra-crystalline fraction of protein, which appeared to adhere to closed-system behaviour in the 3AL shell portion. The 'nacreous' layer did not adhere well to closed-system behaviour, possibly due to complications arising from difficulties sampling the very thin shell (~250 μm thick) and potential mineral diagenesis during drilling. We therefore recommend using the 3AL shell portion for further research involving achatinid shells. Predictable protein degradation, in terms of racemisation and hydrolysis, was observed during elevated temperature experiments, with respect to both temperature and time. Different relative rates of racemisation were observed for proteins in the 'nacreous' layer and 3AL in modern shells for different elevated temperatures, and showed a different pattern of behaviour in the fossils. This prevented accurate extrapolation of fossil parameters from mathematical modelling of high-temperature kinetic experiments. Although numerical dating of Achatininae fossils using two kinetic models was not possible, the consistent degradation patterns and closed-system behaviour of the 3AL shell portion showed that this shell type has the potential to provide chronological data on Pleistocene timescales for many regions across the African continent. Such frameworks would be highly beneficial to archaeologists and Quaternary scientists working at timescales beyond the reach of radiocarbon dating, and in areas of Africa where ostrich eggshell is not present. A larger study of well-constrained fossils from sequences across the region is required to test the full feasibility of Achatininae shells for amino acid geochronology.

Declaration of competing interest

The authors declare that they have no known competing financial interests or personal relationships that could have appeared to influence the work reported in this paper.

Data availability

Data in this study has been included in the supplementary information and will be available on the NOAA data repository.

Acknowledgements

This work was supported by the Natural Environment Research Council [NE/S00713X/1], European Research Council (ERC) under the European Union's Horizon 2020 research and innovation program (grant agreement No 856488) and the fieldwork in Zambia was funded by the National Geographic Society [GEFNE38-12]. We would like to thank Constance Mulenga and Clare Mateke at the Livingstone Museum, Zambia for providing registration numbers and curatorial assistance. Photographs included in Fig. 1 were taken by Kevin Webb, Natural History Museum Publishing and Image Resources, © Trustees of the Natural History Museum, London. We also acknowledge Sheila Taylor and Samantha Presslee for technical support, and Marc Dickinson for helpful comments on an earlier version of this manuscript.

Appendix A. Supplementary data

Supplementary data to this article can be found online at https://doi.org/10.1016/j.quageo.2023.101473.

References

Abelson, P.H., 1955. Organic constituents of fossils. Carnegie Inst. Wash. Year Book 54, 107–109.

Bada, J.L., 1972. Kinetics of racemization of amino acids as a function of pH. Journal of the American Chemical Society 94 (4), 3–1371.

Bada, J.L., Schroeder, R.A., 1972. Racemization of isoleucine in calcareous marine sediments: kinetics and mechanism. Earth Planet Sci. Lett. 15 (1), 1.

Bada, J.L., Shou, M.Y., Man, E.H., Schroeder, R.A., 1978. Decomposition of hydroxy amino acids in foraminiferal tests; kinetics, mechanism and geochronological implications. Earth Planet Sci. Lett. 41 (1), 67–76.

Barham, L.S., Simms, M., Gilmour, M., Debenham, N., 2000. Chapter 10: Twin Rivers, excavation and behavioural record. In: Barham, L.S. (Ed.), The Middle Stone Age of Zambia, South Central Africa. Western Academic & Specialist Press, pp. 165–216.

Bosch, M.D., Mannino, M.A., Prendergast, A.L., O'Connell, T.C., Demarchi, B., Taylor, S. M., Niven, L., Van Der Plicht, J., Hublin, J.J., 2015. New chronology for Ksâr 'Akil (Lebanon) supports Levantine route of modern human dispersal into Europe. Proc. Natl. Acad. Sci. USA 112 (25), 7683–7688.

Bowen, D.Q., Hughes, S., Sykes, G.A., Miller, G.H., 1989. Land-sea correlations in the Pleistocene based on isoleucine epimerization in non-marine molluscs. Nature 340 (6228), 49–51.

Brand, U., Morrison, J.O., 1987. Paleoscene# 6. Biogeochemistry of fossil marine invertebrates. Geosci. Can. 14 (2), 85–107.

Brooks, A.S., Hare, P.E., Kokis, J.E., Miller, G.H., Ernst, R.D., Wendorf, F., 1990. Dating Pleistocene archeological sites by protein diagenesis in ostrich eggshell. Science 248 (4951), 60–64.

Canoira, L., García-Martínez, M.J., Llamas, J.F., Ortíz, J.E., Torres, T.D., 2003. Kinetics of amino acid racemization (epimerization) in the dentine of fossil and modern bear teeth. Int. J. Chem. Kinet. 35 (11), 576–591.

Chaki, K.K., Misra, K.K., Sur, R.K., 1992. The surface morphology of the shell in active and in aestivating *Achatina fulica* (Bowdich) and *Pila globosa* (Swainson). Proc. 9th Eur. Malac. Cong. 97–102.

Clarke, S.J., Murray-Wallace, C.V., 2006. Mathematical expressions used in amino acid racemisation geochronology—a review. Quat. Geochronol. 1 (4), 261–278.

Crisp, M., Demarchi, B., Collins, M., Morgan-Williams, M., Pilgrim, E., Penkman, K., 2013. Isolation of the intra-crystalline proteins and kinetic studies in *Struthio camelus* (ostrich) eggshell for amino acid geochronology. Quat. Geochronol. 16, 110–128.

de Paula, S.M., Silveira, M., 2009. Studies on molluscan shells: contributions from microscopic and analytical methods. Micron 40 (7), 669–690.

Demarchi, B., Rogers, K., Fa, D.A., Finlayson, C.J., Milner, N., Penkman, K.E., 2013a. Intra-crystalline protein diagenesis (IcPD) in *Patella vulgata*. Part I: isolation and testing of the closed system. Quat. Geochronol. 16, 144–157.

Demarchi, B., Collins, M., Bergstrom, E., Dowle, A., Penkman, K., Thomas-Oates, J., Wilson, J., 2013b. New experimental evidence for in-chain amino acid racemization of serine in a model peptide. Anal. Chem. 85 (12), 5835–5842.

Demarchi, B., Hall, S., Roncal-Herrero, T., Freeman, C.L., Woolley, J., Crisp, M.K., Wilson, J., Fotakis, A., Fischer, R., Kessler, B.M., Rakownikow Jersie-Christensen, R., et al., 2016. Protein sequences bound to mineral surfaces persist into deep time. Elife 5, e17092.

Demarchi, B., Clements, E., Coltorti, M., Van De Locht, R., Kröger, R., Penkman, K., Rose, J., 2015. Testing the effect of bleaching on the bivalve *Glycymeris*: a case study of amino acid geochronology on key Mediterranean raised beach deposits. Quat. Geochronol. 25, 49–65.

Dickinson, M.R., Lister, A.M., Penkman, K.E., 2019. A new method for enamel amino acid racemization dating: a closed system approach. Quat. Geochronol. 50, 29–46.

Ellis, G.L., Goodfriend, G.A., Abbott, J.T., Hare, P.E., Von Endt, D.W., 1996. Assessment of integrity and geochronology of archaeological sites using amino acid racemization in land snail shells: examples from central Texas. Geoarchaeology 11 (3), 189–213.

Feng, Q.L., Zhu, X., Li, H.D., Kim, T.N., 2001. Crystal orientation regulation in ostrich eggshells. J. Cryst. Growth 233 (3), 548–554.

Fontanilla, I.K., 2010. *Achatina* (*Lissachatina*) *fulica* Bowdich: its Molecular Phylogeny, Genetic Variation in Global Populations, and its Possible Role in the Spread of the Rat Lungworm Angiostrongylus Cantonensis (Chen). (Doctoral dissertation, University of Nottingham).

Foster, L.C., Andersson, C., Høie, H., Allison, N., Finch, A.A., Johansen, T., 2008. Effects of micromilling on $\delta^{18}O$ in biogenic aragonite. Geochemistry, Geophysics, Geosystems 9 (4).

Goodfriend, G.A., 1991. Patterns of racemization and epimerization of amino acids in land snail shells over the course of the Holocene. Geochem. Cosmochim. Acta 55 (1), 293–302.

Goodfriend, G.A., Hare, P.E., Druffel, E.R.M., 1992. Aspartic-acid racemization and protein diagenesis in corals over the last 350 years. Geochem. Cosmochim. Acta 56, 3847–3850.

Hammouda, S.A., Kadolsky, D., Adaci, M., Mebrouk, F., Bensalah, M., Mahboubi, M.H., Tabuce, R., 2017. Taxonomic review of the "bulimes", terrestrial gastropods from the continental Eocene of the Hamada de Méridja (northwestern Sahara, Algeria) (Mollusca: Stylommatophora: Strophocheilidae?), with a discussion of the genera of the family Vidaliellidae. PalZ 91, 85–112.

Hare, P.E., 1963. Amino acids in the proteins from aragonite and calcite in the shells of *Mytilus californianus*. Science 139 (3551), 216–217.

Hare, P., Mitterer, R., 1967. Non-protein Amino Acids in Fossil Shells. Carnegie Institution of Washington Year Book.

Haugen, J.E., Sejrup, H.P., 1990. Amino acid composition of aragonitic concholin in the shell of *Arctica islandica*. Lethaia 23 (2), 133–141.

Hausdorf, B., 2018. The giant African snail *Lissachatina fulica* as potential index fossil for the Anthropocene. Anthropocene 23, 1–4.

Hearty, P.J., Kaufman, D.S., 2009. A *Cerion*-based chronostratigraphy and age model from the central Bahama Islands: amino acid racemization and ^{14}C in land snails and sediments. Quat. Geochronol. 4 (2), 148–159.

Hearty, P.J., Olson, S.L., 2010. Geochronology, biostratigraphy, and changing shell morphology in the land snail subgenus *Poecilozonites* during the Quaternary of Bermuda. Palaeogeography Palaeoclimatology Palaeoecology 293, 9–29.

Hendy, E.J., Tomiak, P.J., Collins, M.J., Hellstrom, J., Tudhope, A.W., Lough, J.M., Penkman, K.E., 2012. Assessing amino acid racemization variability in coral intra-crystalline protein for geochronological applications. Geochem. Cosmochim. Acta 86, 338–353.

Hill, R.L., 1965. Hydrolysis of proteins. Adv. Protein Chem. 20, 37–107.

Hodasi, J.K.M., 1984. Some Observations on the Edible Giant Land Snails of West Africa. World Animal Review (FAO).

Kaufman, D.S., Manley, W.F., 1998. A new procedure for determining DL amino acid ratios in fossils using reverse phase liquid chromatography. Quat. Sci. Rev. 17 (11), 987–1000.

Kaufman, D.S., 2006. Temperature sensitivity of aspartic and glutamic acid racemization in the foraminifera *Pulleniatina*. Quat. Geochronol. 1 (3), 188–207.

Kimber, R.W., Griffin, C.V., 1987. Further evidence of the complexity of the racemization process in fossil shells with implications for amino acid racemization dating. Geochem. Cosmochim. Acta 51 (4), 839–846.

Kosnik, M.A., Kaufman, D.S., Hua, Q., 2008. Identifying outliers and assessing the accuracy of amino acid racemization measurements for geochronology: I. Age calibration curves. Quat. Geochronol. 3 (4), 308–327.

Kowalewska-Groszkowska, M., Mierzwa-Szymkowiak, D., Zdunek, J., 2018. The crossed-lamellar structure of mollusk shells as biocomposite material. Composites Theory and Practice 18 (2), 71–76.

Kriausakul, N., Mitterer, R.M., 1978. Isoleucine epimerization in peptides and proteins: kinetic factors and application to fossil proteins. Science 201 (4360), 1011–1014.

Lesbani, A., Tamba, P., Mohadi, R., Fahmariyanti, F., 2013. Preparation of calcium oxide from *Achatina fulica* as catalyst for production of biodiesel from waste cooking oil. Indonesian Journal of Chemistry 13 (2), 176–180.

Mead, A.R., 1991. Anatomical criteria in the systematics of the Achatinidae (Pulmonata). In: Proceedings of the 10th International Malacological Congress, Meier-Brook C. Tubingen, pp. 549–553.

Miller, G.H., Beaumont, P.B., Jull, A.J., Johnson, B., 1992. Pleistocene geochronology and palaeothermometry from protein diagenesis in ostrich eggshells: implications for the evolution of modern humans. Phil. Trans. Roy. Soc. Lond. B Biol. Sci. 337 (1280), 149–157.

Millman, E., Wheeler, L., Billups, K., Kaufman, D., Penkman, K.E., 2022. Testing the effect of oxidizing pre-treatments on amino acids in benthic and planktic foraminifera tests. Quat. Geochronol. 73, 101401.

Mitterer, R.M., Kriausakul, N., 1984. Comparison of rates and degrees of isoleucine epimerization in dipeptides and tripeptides. Org. Geochem. 7 (1), 91–98.

Murray-Wallace, C.V., 1995. Aminostratigraphy of Quaternary coastal sequences in southern Australia—an overview. Quat. Int. 26, 69–86.

Murray-Wallace, C.V., Richter, J., Vogelsang, R., 2015. Aminostratigraphy and taphonomy of ostrich eggshell in the sedimentary infill of Apollo 11 Rockshelter, Namibia. J. Archaeol. Sci.: Report 4, 143–151.

Neubert, E., van Damme, D., 2012. Palaeogene Continental Molluscs of Oman. Naturhistorisches Museum der Burgergemeinde Bern.

New, E., Yanes, Y., Cameron, R.A., Miller, J.H., Teixeira, D., Kaufman, D.S., 2019. Aminochronology and time averaging of Quaternary land snail assemblages from colluvial deposits in the Madeira Archipelago, Portugal. Quat. Res. 92 (2), 483–496.

Ortiz, J.E., Torres, T., Yanes, Y., Castillo, C., Nuez, J.D., Ibáñez, M., Alonso, M.R., 2006. Climatic cycles inferred from the aminostratigraphy and aminochronology of Quaternary dunes and palaeosols from the eastern islands of the Canary Archipelago. J. Quat. Sci.: Published for the Quaternary Research Association 21 (3), 287–306.

Ortiz, J.E., Torres, T., Pérez-González, A., 2013. Amino acid racemization in four species of ostracodes: taxonomic, environmental, and microstructural controls. Quat. Geochronol. 16, 129–143.

Ortiz, J.E., Gutiérrez-Zugasti, I., Torres, T., González-Morales, M., Sánchez-Palencia, Y., 2015. Protein diagenesis in *Patella* shells: implications for amino acid racemisation dating. Quat. Geochronol. 27, 105–118.

Ortiz, J.E., Torres, T., Sánchez-Palencia, Y., Ferrer, M., 2017. Inter-and intra-crystalline protein diagenesis in *Glycymeris* shells: implications for amino acid geochronology. Quat. Geochronol. 41, 37–50.

Ortiz, J.E., Sánchez-Palencia, Y., Gutiérrez-Zugasti, I., Torres, T., González-Morales, M., 2018. Protein diagenesis in archaeological gastropod shells and the suitability of this material for amino acid racemisation dating: *Phorcus lineatus* (da Costa, 1778). Quat. Geochronol. 46, 16–27.

Penkman, K.E.H., 2005. Amino Acid Geochronology: a Closed System Approach to Test and Refine the UK Model, Unpubl PhD Thesis. Univ Newcastle.

Penkman, K.E.H., Kaufman, D.S., Maddy, D., Collins, M.J., 2008. Closed-system behaviour of the intra-crystalline fraction of amino acids in mollusc shells. Quat. Geochronol. 3 (1–2), 2–25.

Penkman, K.E.H., Preece, R.C., Keen, D.H., Maddy, D., Schreve, D.C., Collins, M.J., 2007. Testing the aminostratigraphy of fluvial archives: the evidence from intra-crystalline proteins within freshwater shells. Quat. Sci. Rev. 26 (22–24), 2958–2969.

Penkman, K.E.H., Preece, R.C., Keen, D.H., Collins, M.J., 2010. Amino acid geochronology of the type Cromerian of West Runton, Norfolk, UK. Quat. Int. 228 (1–2), 25–37.

Pickford, M., 1995. Fossil land snails of East Africa and their palaeoecological significance. J. Afr. Earth Sci. 20 (3–4), 167–226.

Pickford, M., 2008. Freshwater and Terrestrial Mollusca from the Early Miocene Deposits of the Northern Sperrgebiet, Namibia, vol. 20. Memoir of the Geological Survey of Namibia, pp. 65–74.
Pickford, M., Senut, B., Mocke, H., Mourer-Chauviré, C., Rage, J.C., Mein, P., 2014. Eocene aridity in southwestern Africa: timing of onset and biological consequences. Trans. Roy. Soc. S. Afr. 69 (3), 139–144.
Pierini, F., Demarchi, B., Turner, J., Penkman, K., 2016. *Pecten* as a new substrate for IcPD dating: the Quaternary raised beaches in the Gulf of Corinth, Greece. Quat. Geochronol. 31, 40–52.
Powell, J., Collins, M.J., Cussens, J., MacLeod, N., Penkman, K.E., 2013. Results from an amino acid racemization inter-laboratory proficiency study; design and performance evaluation. Quat. Geochronol. 16, 183–197.
Preece, R.C., Penkman, K.E.H., 2005. New faunal analyses and amino acid dating of the Lower Palaeolithic site at East Farm, Barnham, Suffolk. Proc. Geologists' Assoc. 116 (3–4), 363–377.
Raut, S.K., Barker, G.M., 2002. *Achatina fulica* Bowdich and Other Achatinidae as Pests in Tropical Agriculture. In: Molluscs as Crop Pests. CAB International, Wallingford, United Kingdom, pp. 55–114.
Roberts, D.L., Bateman, M.D., Murray-Wallace, C.V., Carr, A.S., Holmes, P.J., 2008. Last interglacial fossil elephant trackways dated by OSL/AAR in coastal aeolianites, Still Bay, South Africa. Palaeogeography, Palaeoclimatology, Palaeoecology 257 (3), 79–261.
Simms, M.J., 2000. Appendix 7(a): Preliminary report on the sediments of Lake Patrick. In: Barham, L.S. (Ed.), The Middle Stone Age of Zambia, South Central Africa, vol. 2000. Western academic & specialist Press.
Smith, G.G., Williams, K.M., Wonnacott, D.M., 1978. Factors affecting the rate of racemization of amino acids and their significance to geochronology. J. Org. Chem. 43 (1), 1–5.
Smith, G.G., Evans, R.C., 1980. The Effect of Structure and Conditions on the Rate of Racemisation of Free and Bound Amino Acids. In: Hare, P.E., Hoering, T.C., King, K. (Eds.), Biogeochemistry of Amino Acids. John Wiley & Sons, Ltd, New York, pp. 257–282.
Solem, A., 1979. A Theory of Land Snail Biogeographic Patterns through Time. Pathways in Malacology. The Hague: Bohn S. Holkema U, and Junk W, pp. 225–249.
Sykes, G.A., Collins, M.J., Walton, D.I., 1995. The significance of a geochemically isolated intracrystalline organic fraction within biominerals. Org. Geochem. 23 (11–12), 1059–1065.
Taylor, V.K., Barton, R.N., Bell, M., Bouzouggar, A., Collcutt, S., Black, S., Hogue, J.T., 2011. The Epipalaeolithic (Iberomaurusian) at Grotte des Pigeons (Taforalt), Morocco: a preliminary study of the land Mollusca. Quat. Int. 244 (1), 5–14.
Tomiak, P.J., Penkman, K.E., Hendy, E.J., Demarchi, B., Murrells, S., Davis, S.A., McCullagh, P., Collins, M.J., 2013. Testing the limitations of artificial protein degradation kinetics using known-age massive *Porites* coral skeletons. Quat. Geochronol. 16, 87–109.
Torres, T., Ortiz, J.E., Fernández, E., Arroyo-Pardo, E., Grün, R., Pérez-González, A., 2014. Aspartic acid racemization as a dating tool for dentine: a reality. Quat. Geochronol. 22, 43–56.
Towe, K.M., 1980. Preserved organic ultrastructure: an unreliable indicator for Paleozoic amino acid biogeochemistry. In: Hare, P.E., Hoering, T.C., King, K.J. (Eds.), The Biogeochemistry of Amino Acids. Wiley, New York, pp. 65–74.
Vijayan, K., Suganthasakthivel, R., Naggs, F., Fontanilla, I.K., Soorae, P.S., Sajeev, T.V., Wade, C.M., 2022. Fine-scale geographical sampling and molecular characterization of the giant African land snail in its invasive range in Asia shows low genetic diversity, new haplotypes and the emergence of another haplotype from the Indian Ocean Islands. Biol. J. Linn. Soc. 137 (3), 421–433.
Wehmiller, J.F., Stecher, H.A., York, L.L., Friedman, I., 2000. The Thermal Environment of Fossils: Effective Ground Temperatures at Aminostratigraphic Sites on the US Atlantic Coastal Plain. Perspectives in Amino Acid and Protein Geochemistry. Oxford University Press, Oxford, pp. 219–250.
Wehmiller, J.F., Harris, W.B., Boutin, B.S., Farrell, K.M., 2012. Calibration of amino acid racemization (AAR) kinetics in United States mid-Atlantic Coastal Plain Quaternary mollusks using $^{87}Sr/^{86}Sr$ analyses: evaluation of kinetic models and estimation of regional Late Pleistocene temperature history. Quat. Geochronol. 7, 21–36.
Wheeler, L.J., Penkman, K.E., Sejrup, H.P., 2021. Assessing the intra-crystalline approach to amino acid geochronology of *Neogloboquadrina pachyderma* (sinistral). Quat. Geochronol. 61, 101131.
White, T.S., Bridgland, D.R., Limondin-Lozouet, N., Schreve, D.C., 2017. Fossils from Quaternary fluvial archives: sources of biostratigraphical, biogeographical and palaeoclimatic evidence. Quat. Sci. Rev. 166, 150–176.
Wojcieszak, M., Backwell, L., d'Errico, F., Wadley, L., 2023. Evidence for large land snail cooking and consumption at Border Cave c. 170–70 ka ago. Implications for the evolution of human diet and social behaviour. Quat. Sci. Rev. 306, 108030.